Asia Pac. J. Math. 2026 **13**:16

GENERALIZED SHIFTED LAPLACE PRECONDITIONER FOR THE HIGH-FREQUENCY ACOUSTIC SCATTERING PROBLEM

IBRAHIM ZANGRÉ[1,*], DAOUDA PARÉ[2], WENDDABO OLIVIER SAWADOGO[3]

[1]Université Thomas SANKARA, Laboratoire Sciences et Technologie (LaST), Burkina Faso

[2]Université Norbert ZONGO, Laboratoire de Mathématiques, Informatique et Applications (L@MIA), Burkina Faso

[3]Université Lédéa Bernard OUÉDRAOGO, Laboratoire de Recherche et Développement (LaReD), Burkina Faso

[*]Corresponding author: ibzangre@gmail.com

Received Dec. 6, 2025

Abstract. The iterative solution of linear systems arising from wave scattering is a difficult and challenging problem, especially in the high frequency regime. Over the last two decades many preconditioning techniques have been proposed to improve the convergence of iterative solvers; one of the most successful being the Shifted Laplace Preconditioner. The aim of this paper is to propose a generalization of the Shifted Laplace Preconditioner by using operator representation combined with complex Padé approximants. The resulting method is a family of Generalized Shifted Laplace Preconditioners and provides promising results for two- and three-dimensional scattering problems, and that it leads to convergence rates that are weakly frequency-dependent. In the symbolic calculus of pseudodifferential operators, the lowest order member of this new family of preconditioners corresponds to the standard Shifted Laplace Preconditioner.

2020 Mathematics Subject Classification. 35J05; 65N30; 65F08; 65L20.

Key words and phrases. wave scattering; Helmholtz equation; high frequency; Krylov subspace method; preconditioners.

1. Introduction

Solving large-scale time-harmonic acoustic scattering problems remains a challenging problem, in particular in the *high frequency regime* [38, 39]. Various methods can be designed to attack the problem solution, each one having its pros and cons. Among the most widely used methods, let us mention integral equations techniques [3, 32] and volumetric methods [3, 13, 40] in conjunction with non-reflecting boundary conditions or PMLs [3]. The aim of this paper is to contribute to the iterative numerical solution of the linear system related to volumetric approaches. More particularly, we propose the construction of a new class of robust and efficient preconditioners for the Krylov subspace solution [34] of the associated linear system.

DOI: 10.28924/APJM/13-16

It is well-known that the spectral properties of the matrix $\mathbb{H}_h$ associated with the discretization of the exterior Helmholtz equation makes extremely difficult and sometimes impossible the convergence of the iterative solvers applied to the related linear system [38, 39]. Indeed, $\mathbb{H}_h$ is complex-valued, often symmetric, but *highly indefinite*. This last point is related to the fact that the matrix is associated with the Helmholtz operator $\mathcal{H} := -(\Delta + k^2)$. Therefore, the indefinite character of $\mathcal{H}$ implies the same property at the discrete level (e.g. after a finite element discretization) for $\mathbb{H}_h$, the situation deteriorating as the wavenumber k increases. For many years much effort has been directed towards the construction and implementation of robust and efficient preconditioners for designing convergent Krylov subspace solvers. The most common approach is purely algebraic in the sense that, being given a discrete representation $\mathbb{H}_h$ of the operator $\mathcal{H}$, a preconditioner is built from the entries of $\mathbb{H}_h$ by advanced algebraic techniques. Without being exhaustive, let us mention for example the algebraic multilevel preconditioners [7], ILUT [29, 33] and also pARMS [33] methods. Let us also point out here that alternative methods based on Domain Decomposition Methods [8, 22, 26, 38] can be derived to get adapted preconditioners or solvers.

In parallel to these algebraic preconditioners, physics-based or analytical preconditioners have been proposed recently. The main idea is to include information related to the physical properties of the problem or/and to the analytical structure of the operator $\mathcal{H}$ when trying to build a preconditioner. Among the main contributions, let us mention AILU preconditioners [23, 39], Shifted Laplace Preconditioners [12, 20, 39], fast sweeping preconditioners [15], and more recently deep learning based-techniques [4]. In particular, Shifted Laplace Preconditioners (SLP), which are improved versions of Bayliss, Goldstein & Turkel's Laplace preconditioner [6], have received much attention during the last few years. Essentially, a preconditioner is built based on a complex version of the Helmholtz equation and approximated *via* ILU or multigrid methods since definite positiveness has been reinforced through the introduction of a fictitious dissipative term into the equation. The approach has been applied successfully to various wave-like problems [1, 11, 16, 17, 20, 21, 28, 36]: acoustics, electromagnetism, elasticity, unbounded domains, heterogeneous media... However, even if SLP methods provide great expectations, some problems remain. For example, the convergence of Krylov solvers is still frequency-dependent even for simple geometrical configurations, which limits SLP application to moderate wavenumbers for three-dimensional problems. Extremely slow convergence can also be encountered for resonant structures. Furthermore, the choice of the optimal damping parameter is closely related to some numerical studies.

The aim of this paper is to propose a general construction of Generalized Shifted Laplace Preconditioners (called GSLP) based on analytical operator theory, rational approximants and hybridization with algebraic approaches (ILUT in the present paper). In particular, the GSLP proposed here lead to weak convergence dependence (and sometimes independence) of the Krylov solver with respect

to the wavenumber k and mesh refinement. Finally, GSLP are a high-order generalization of SLP since the lowest-order GSLP approximation gives SLP. For this reason, adapting SLP to GSLP is a very simple task, whatever the approximation method (Finite Difference, Finite Element,...), since the preconditioner construction is only based on elementary bricks of SLP plus rational approximation coefficients that we provide here.

The plan of the paper is the following. In Section 2, we set up the scattering problem and its approximation by using a local absorbing boundary condition and finite element approximation. Section 3 proposes an original point of view to understand the continuous spectral properties of SLP based on pseudodifferential operators theory. We also describe its discretization in Subsection 3.1 as well as how to choose the associated absorbing boundary condition for a weak variational approximation (Subsection 3.2). Section 4 introduces the Generalized Shifted Laplace Preconditioners. We first explain in Subsection 4.1 how to build an analytical continuous inverse operator of $\mathcal{H}$ by using nonlocal pseudodifferential square-root operators. Then, in Subsection 4.3, we propose a suitable localization of these operators with the help of Padé approximants (Subsection 4.2). Subsection 4.4 deals with the algebraic representation of HSLP in a variational formulation framework, well-adapted to the finite element approximation. We develop a numerical study of the spectral properties of GSLP in Subsection 4.5. This analysis is important for understanding what can be expected from our approach in terms of convergence of a Krylov solver (GMRES in the paper). Section 5 presents a thorough numerical study of HSLP compared to SLP for different two- and three-dimensional objects. In particular, we numerically prospect the dependence of the convergence rate of the preconditioned solvers with respect to the wavenumber k, the discretization density and the geometrical features. Furthermore, we numerically analyze the effect of the coupling of the analytical preconditioners with ILUT methods to sparsify the matrix representations. Finally, Section 6 draws a conclusion and points out some forthcoming issues with regard to the present paper.

2. Approximation of the Acoustic Scattering Problem

We consider the time-harmonic scattering problem of an incident acoustic wave u^{inc} by a bounded obstacle $\Omega^- \subset \mathbb{R}^d$ $(d = 2, 3)$ with boundary $\Gamma := \partial\Omega^-$. The scattered field u propagates in the unbounded domain $\Omega^+ = \mathbb{R}^d \setminus \overline{\Omega^-}$ and is solution to the exterior Helmholtz problem with Dirichlet boundary condition

$$\begin{cases} -\Delta u - k^2 u = 0 \text{ in } \Omega^+, \\ u = -u^{\text{inc}} \text{ on } \Gamma, \\ \lim\limits_{|\mathbf{x}|\to\infty} |\mathbf{x}|^{\frac{d-1}{2}} \left(\nabla u \cdot \dfrac{\mathbf{x}}{|\mathbf{x}|} - \imath k u \right) = 0. \end{cases} \tag{1}$$

In the above system, $|\mathbf{x}|$ is the Euclidean norm of $\mathbf{x} = (x_1, \cdots, x_d) \in \mathbb{R}^d$, $\imath = \sqrt{-1}$ is the imaginary unit and k denotes the wavenumber related to the wavelength λ of the incident wave through $k = 2\pi/\lambda$. In

what follows, choosing a Dirichlet boundary condition (sound-soft case) on Γ is not restrictive and any other boundary condition could have been considered. The last equation of system (1) is the so-called Sommerfeld radiation condition at infinity which ensures that the scattered wave is outgoing and imposes the uniqueness of the solution.

One of the difficulties when solving scattering problems is that we have to deal with an unbounded domain. For numerical purposes, we introduce an Absorbing Boundary Condition (ABC) [14] on a fictitious boundary Γ^∞. Therefore, we have to solve a Helmholtz-type problem in the bounded computational domain Ω (delimited by Γ^∞ and Γ)

$$\begin{cases} -\Delta u - k^2 u &= 0 \text{ in } \Omega, \\ u &= -u^{\text{inc}} \text{ on } \Gamma, \\ \partial_{\mathbf{n}} u + \mathcal{B} u &= 0 \text{ on } \Gamma^\infty, \end{cases} \tag{2}$$

where $\mathbf{n}$ is the outwardly directed unit normal vector to Γ^∞ and $\mathcal{B}$ is an approximation of the Dirichlet-to-Neumann operator. In the rest of the paper, we will only consider the Sommerfeld (lowest order ABC) boundary condition:

$$\mathcal{B} = -\imath k. \tag{3}$$

(High-order order ABCs or other truncation techniques like Perfectly Matched Layers could have been considered as well.) The variational formulation of (2) then writes: Find $u \in H^1(\Omega)$ with $u|_\Gamma = -u^{\text{inc}}|_\Gamma$ such that

$$\int_\Omega \left(\nabla u \cdot \nabla v - k^2 uv\right) d\mathbf{x} - \imath k \int_{\Gamma^\infty} uv d\sigma = 0, \quad \forall v \in H_0^1(\Omega). \tag{4}$$

Let $\mathbb{S}_h$ be the stiffness matrix, $\mathbb{M}_h$ the mass matrix and $\mathbb{B}_h$ the surface mass matrix (on Γ^∞) arising from the $\mathbb{P}_1$ Finite Element Method (FEM) discretization of (4). The small parameter h is the mesh size. Let n_h be the total number of degrees of freedom of the FEM and $n_\lambda := \lambda/h$ the density of discretization points per wavelength. We define $\mathbf{u}_h \in \mathbb{C}^{n_h}$ as the discrete unknown vector and $\mathbf{b}_h \in \mathbb{C}^{n_h}$ the right-hand side related to the discretization of the incident plane wave by the FEM. This finally results in the solution of the linear system of equations

$$\mathbb{H}_h \mathbf{u}_h := \left(\mathbb{S}_h - k^2 \mathbb{M}_h - \imath k \mathbb{B}_h\right) \mathbf{u}_h = \mathbf{b}_h. \tag{5}$$

3. Shifted Laplace Preconditioners (SLP)

It is well-known that solving (5) iteratively, e.g. with Krylov-subspace methods, is challenging. This is mainly due to the fact that the sparse complex-valued matrix $\mathbb{H}_h$ is highly indefinite, most particularly for large wave numbers or/and for fine computational grids. Practically, the complex eigenvalues of the matrix $\mathbb{H}_h$ spread out in the complex plane, some having a positive and others a negative real part. As a consequence, Krylov subspace iterative solvers [35] diverge or exhibit extremely slow convergence rates. This implies that preconditioners are required to get or improve the convergence. During the last

few years, a particular attention has been directed towards Shifted Laplace Preconditioners (SLP) [18]. To get increased definite positiveness from the preconditioners, the Helmholtz operator $\mathcal{H} = -\Delta - k^2$ is rescaled by a complex wave number resulting in the damped Helmholtz operator $\mathcal{A}_{(\alpha)} = -\Delta - \alpha k^2$, $\alpha = a + \imath b \in \mathbb{C}$. The shifted Laplace operator $\mathcal{A}_{(\alpha)}$ leads to suitable preconditioners since adding an artificial dissipative term implies that 1) $\mathcal{A}_{(\alpha)}$ can be solved efficiently by using ILU factorizations or multigrid methods [16, 18–20] and 2) robustness is highly increased thanks to a clustering of the eigenvalues in the complex plane for the preconditioned linear system. To the best of our knowledge, this last property is always presented in the SLP literature as an algebraic property. We want to point out here that this in fact results from a simple symbolic property of the composition rule of the operators $\mathcal{A}_{(\alpha)}$ and $\mathcal{H}$ *at the continuous level*. This will serve as our basis for designing high-order generalizations of SLP in Section 4.

3.1. **SLP: spectral properties at the continuous level.** Let us consider the Helmholtz operator $\mathcal{H}$ in the whole space $\mathbb{R}^d$ and $\mathcal{A}_{(\alpha)}$ the associated shifted Helmholtz operator. In order to analyze their spectral properties at the continuous level, we diagonalize them in Fourier space. If we define $\boldsymbol{\xi} = (\xi_1, \cdots, \xi_d) \in \mathbb{R}^d$ as the Fourier covariable, the symbols [10, 37] of $\mathcal{H}$ and $\mathcal{A}_{(\alpha)}$ are respectively

$$\sigma_{[\mathcal{H}]}(\boldsymbol{\xi}) = |\boldsymbol{\xi}|^2 - k^2 \quad \text{and} \quad \sigma_{[\mathcal{A}_{(\alpha)}]}(\boldsymbol{\xi}) = |\boldsymbol{\xi}|^2 - \alpha k^2, \quad \forall \boldsymbol{\xi} \in \mathbb{R}^d. \tag{6}$$

These symbols can be roughly seen as a "continuous" spectral version of the "discrete" algebraic eigenvalues. The symbol of the preconditioned operator $\mathcal{A}_{(\alpha)}^{-1}\mathcal{H}$ is then

$$\sigma_{[\mathcal{A}_{(\alpha)}^{-1}\mathcal{H}]}(z) = \frac{|\boldsymbol{\xi}|^2 - k^2}{|\boldsymbol{\xi}|^2 - \alpha k^2} = \frac{1+z}{\alpha + z}, \quad \forall z = -\frac{|\boldsymbol{\xi}|^2}{k^2} \in \mathbb{R}^-. \tag{7}$$

Let us consider now the complex Poincaré map

$$\begin{aligned} \sigma_{[\mathcal{A}_{(\alpha)}^{-1}\mathcal{H}]} : \mathbb{R}^- &\to \mathcal{C}_{(\alpha)} \\ z &\mapsto \sigma_{[\mathcal{A}_{(\alpha)}^{-1}\mathcal{H}]}(z) \end{aligned} \tag{8}$$

This application $\sigma_{[\mathcal{A}_{(\alpha)}^{-1}\mathcal{H}]}$ transforms $\mathbb{R}^-$ into the domain $\mathcal{C}_{(\alpha)}$ which is the clockwise directed circular arc of center

$$\frac{1}{2} + \imath \frac{a-1}{2b}$$

and of radius

$$\sqrt{\frac{1}{4} + \frac{(a-1)^2}{4b^2}},$$

with endpoints α^{-1} and $(1, 0)$ (see Figure 1). The geometrical description of $\mathcal{C}_{(\alpha)}$ can be related to physics/operator interpretation in the following way. The first endpoint α^{-1} is obtained for the zero spatial frequency: $\boldsymbol{\xi} = 0$ (and $z = 0$). Then, for the set of low spatial frequencies $\mathbf{H} := \{(k, \boldsymbol{\xi}) \in \mathbb{R} \times \mathbb{R}^d / |\boldsymbol{\xi}| < k\}$, the arc extends from α^{-1} to the origin $(0, 0)$ for $\mathbf{G} := \{(k, \boldsymbol{\xi}) \in \mathbb{R} \times \mathbb{R}^d / |\boldsymbol{\xi}| \approx k\}$ (and $z \approx -1$). Finally, for high spatial frequencies $\mathbf{E} :=$

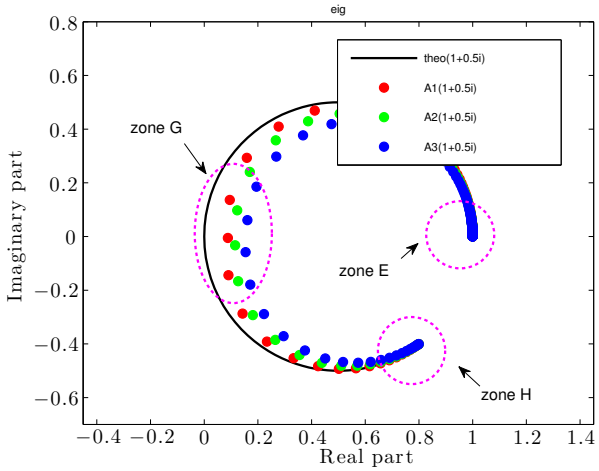

FIGURE 1. Distribution of the eigenvalues of the preconditioned Helmholtz operator. The black curve represents the analytic arc. The colored dots represent the discrete spectrum for the different versions of SLP ($k = 20\pi$, $n_\lambda = 80$, $\alpha = 1 + \frac{1}{2}\imath$).

$\{(k, \boldsymbol{\xi}) \in \mathbb{R} \times \mathbb{R}^d / |\boldsymbol{\xi}| > k\}$, the arc goes from the origin to the endpoint $(1, 0)$ ($z \to -\infty$). The sets **H** and **E** are generally called [37] the hyperbolic and elliptic zones of the Helmholtz operator $\mathcal{H}$ and correspond to physical propagative and evanescent modes, respectively. The zone **G** is the transition zone from the hyperbolic to the elliptic part.

Contrary to the spectrum of the unpreconditioned Helmholtz operator $\mathcal{H}$, all the eigenvalues of $\mathcal{A}_{(\alpha)}^{-1}\mathcal{H}$ have a positive real part, which ensures the convergence of an iterative solver. In addition, the eigenvalues related to **H** (respectively **E**) cluster at α^{-1} (respectively $(1, 0)$) when $z \to 0$ (respectively $z \to -\infty$). This means that, after discretization of the preconditioned operator $\mathcal{A}_{(\alpha)}^{-1}\mathcal{H}$, the convergence of an iterative Krylov subspace solver should be strongly accelerated —most particularly with respect to the frequency (related to the zone **H**) and the density of discretization points per wavelength n_λ (related to the zone **E**). However, small eigenvalues near the origin for the zone **G** should penalize the convergence, essentially with respect to the frequency.

According to this analysis, we can conclude that the convergence of an iterative Krylov subspace solver applied to the linear system with SLP will be independent of the mesh refinement and dependent (but in a weaker way than without the preconditioner) of the wave number k. The convergence is also clearly affected by the choice of the α parameter. Following extensive studies in the literature [16,18], we propose the "optimal" choice of the complex shift $\alpha = 1 + \frac{1}{2}\imath$ obtained through numerical simulations. We will explain below how this optimal parameter naturally arises in our generalization of SLP.

3.2. **SLP: boundary conditions.** Before proceeding to this generalization, let us point out that the above analysis, made in the whole space $\mathbb{R}^d$, could be extended to handle the contribution of the boundary condition on the scattering surface Γ. However, this would require the use of quite technical

mathematical analysis tools based on pseudodifferential operators [2, 10, 37], microlocal analysis and associated symbolic calculus, which is out of the scope of this paper. Roughly speaking, let us simply state that our analysis formally extends near the boundary if one considers the tangent plane approximation which locally looks like the half-space case. Furthermore, we will impose on Γ the boundary condition corresponding to the physical boundary related to (1), that is the Dirichlet boundary condition here.

Finally, let us stress that in a bounded computational domain, the question arises as to which (if any) boundary condition should be considered on Γ^∞ for the construction of $\mathcal{A}_{(\alpha)}$. One first choice could be to use the same ABC (3) as for the original problem, that is, to consider the following discrete SLP

$$\mathbb{A}^{\imath k}_{(\alpha),h} := \mathbb{S}_h - \alpha k^2 \mathbb{M}_h - \imath k \mathbb{B}_h. \tag{9}$$

However, since we are dealing with a damping Helmholtz operator with complex wave number $\sqrt{\alpha}k$, it seems more natural to rather consider the ABC for the fictitious dissipative media

$$\partial_{\mathbf{n}} u = \imath\sqrt{\alpha} k u \text{ on } \Gamma^\infty \tag{10}$$

and the associated SLP

$$\mathbb{A}^{\imath\sqrt{\alpha}k}_{(\alpha),h} := \mathbb{S}_h - \alpha k^2 \mathbb{M}_h - \imath\sqrt{\alpha} k \mathbb{B}_h. \tag{11}$$

An illustration of these two choices is given in Figure 1. We consider an incident time harmonic wave $u^{\text{inc}} = e^{-\imath k x_1}$ scattering at $\Gamma = \{0\}$. The bounded computational domain is $\Omega = (0, 1)$ and $\Gamma^\infty = \{1\}$. We report the distribution of the eigenvalues of $[\mathbb{A}^{\imath k}_{(\alpha),h}]^{-1}\mathbb{H}_h$ and $[\mathbb{A}^{\imath\sqrt{\alpha}k}_{(\alpha),h}]^{-1}\mathbb{H}_h$. For completeness, we also present the spectrum of the preconditioned matrix $[\mathbb{A}^{0}_{(\alpha),h}]^{-1}\mathbb{H}_h$ corresponding to SLP with a homogeneous Neumann boundary condition on Γ^∞. In each case the preconditioner is inverted exactly. Since the real part of the eigenvalues of $[\mathbb{A}^{\imath\sqrt{\alpha}k}_{(\alpha),h}]^{-1}\mathbb{H}_h$ are the largest, which reinforces the positive definiteness of the preconditioned matrix, we will retain (11) as our reference SLP in what follows.

4. Generalized Shifted Laplace Preconditioner (GSLP)

As seen above, the SLP allows to obtain a preconditioned linear system with eigenvalues lying in the right half-plane. In addition, the shifted Laplace operator itself also has positivity properties, which allows for efficient and stable approximations by e.g. incomplete LU factorizations or multigrid methods. In this section we present a generalization of SLP, called Generalized SLP (GSLP), which is designed to preserve these two fundamental properties while improving on the convergence properties of SLP.

First, preconditioners are built in Subsection 4.1 at the continuous level by using the theory of pseudodifferential operators and associated symbolic calculus. Using the square root operator, positivity properties arise naturally. The resulting implicit preconditioners are however nonlocal, which means that, at the discrete level (after application of the FEM), linear systems associated with full matrices

must be solved. To localize them, we use in Subsection 4.3 well-suited complex Padé approximants (Subsection 4.2) which lead to the solution of *uncoupled* linear systems of equations (Subsection 4.4). In Subsection 4.5, we develop a first numerical study to understand the distribution of the eigenvalues of the preconditioned operators.

The efficient approximate version of the GSLP, where incomplete factorizations are used instead of full LU factorizations to approximate the solution of the uncoupled linear systems, will be analyzed later in Section 5.

4.1. **Analytical inverse preconditioner.** Let us come back to the Helmholtz operator $\mathcal{H}$. Its symbol (6) is a space-independent smooth function, homogeneous of order two with respect to $(k, \boldsymbol{\xi})$. Therefore, this symbol is a classical symbol in $\mathcal{S}^2$ [10,37]. (For heterogeneous media, where k is $\mathbf{x}$-dependent, an adaptation of the theory can be considered but at the price of more technical developments.)

We now propose to compute the pseudodifferential operator $\mathcal{P}$ of order -1 such that

$$\mathcal{P}^2\mathcal{H} = \mathcal{I}, \tag{12}$$

where $\mathcal{I}$ is the identity operator in L^2. The operator $\mathcal{P}^2$ means that we compose $\mathcal{P}$ with itself. Furthermore, $\mathcal{P}^2$ can be seen as the *exact inverse* of $\mathcal{H}$ which would lead to a *convergence in one iteration* when used in a Krylov solver. Unfortunately, this point is *ideal* and computationally unrealistic since $\mathcal{P}$ is the *nonlocal operator* given by

$$\mathcal{P} := \mathcal{H}^{-\frac{1}{2}} = \left[-\Delta - k^2\right]^{-\frac{1}{2}} \tag{13}$$

with symbol

$$\sigma_{[\mathcal{P}]} = \left(|\boldsymbol{\xi}|^2 - k^2\right)^{-\frac{1}{2}} = \frac{1}{ik}(1+z)^{-\frac{1}{2}},\ z = -\frac{|\boldsymbol{\xi}|^2}{k^2} \in \mathbb{R}^-. \tag{14}$$

In the above equation, $\sqrt{z}$ denotes the principal determination of the square-root of a complex number z with branch-cut along the negative real axis. Furthermore, $\sqrt{\mathcal{L}}$ is the square-root of an operator $\mathcal{L}$ which is defined in [37] through the spectral decomposition of $\mathcal{L}$.

Since using (13) directly is unpractical, we can try to localize it. Such localizations of pseudodifferential operators, using Taylor or rational approximants, have been successfully used for the construction of ABCs [2,14], for building well-conditioned integral equations in scattering problems , or for building optimized interface conditions in Domain Decomposition Methods [22]. In particular, *complex Padé rational approximants* have proven to provide excellent approximations to the square-root operator. From (14), in order to provide an implicit local approximation of the operator $\mathcal{P}$, we are thus interested in computing the Padé rational approximants of

$$f_\tau(z) = (1+z)^\tau, \quad \tau \in \mathbb{R}. \tag{15}$$

4.2. **Real and complex Padé rational approximants.** Let $P_\ell(z)$ and $Q_m(z)$ be two polynomials of respective degree ℓ and m. Then, the Padé rational approximants $f_\tau^{[\ell/m]}(z) = P_\ell(z)/Q_m(z)$ of $f_\tau(z)$ accelerate the convergence of the Taylor expansion of $f_\tau(z)$ far from the origin with an order of $(\ell+m+1)$ [5,9,27,30,31].

Being given the function f_τ with its entire series expansion near the origin, we thus want to find the coefficients of $P_\ell(z)$ and $Q_m(z)$ such that

$$f_\tau(z) = \sum_{i=0}^{\infty} c_i z^i = \frac{P_\ell(z)}{Q_m(z)} + \mathcal{O}(z^{\ell+m+1}). \tag{16}$$

Assuming $P_\ell(z) = \mu_0 + \mu_1 z + \cdots + \mu_\ell z^\ell$ and $Q_m(z) = \nu_0 + \nu_1 z + \cdots + \nu_m z^m$, then

$$(\nu_0 + \nu_1 z + \cdots + \nu_m z^m) \sum_{i=0}^{\infty} c_i z^i = \mu_0 + \mu_1 z + \cdots + \mu_\ell z^\ell + \mathcal{O}(z^{\ell+m+1}). \tag{17}$$

Without loss of generality we can set

$$\nu_0 = 1. \tag{18}$$

By equating the coefficients of $z^{\ell+1}, z^{\ell+2}, \cdots, z^{\ell+m}$ in (17) we get the following system of m equations where the unknowns are $\nu_1, \nu_2, \cdots, \nu_m$:

$$\begin{pmatrix} c_{\ell-m+1} & c_{\ell-m+2} & \cdots & c_\ell \\ c_{\ell-m+2} & c_{\ell-m+3} & \cdots & c_{\ell+1} \\ \vdots & \vdots & \ddots & \vdots \\ c_{\ell-1} & c_\ell & \cdots & c_{\ell+m-2} \\ c_\ell & c_{\ell+1} & \cdots & c_{\ell+m-1} \end{pmatrix} \begin{pmatrix} \nu_m \\ \nu_{m-1} \\ \vdots \\ \nu_2 \\ \nu_1 \end{pmatrix} = - \begin{pmatrix} c_{\ell+1} \\ c_{\ell+2} \\ \vdots \\ c_{\ell+m-1} \\ c_{\ell+m} \end{pmatrix}. \tag{19}$$

Since this system has a moderate size, it can be solved by a direct method (e.g. a LU factorization) defining hence the coefficients of $Q_m(z)$ thanks to (18). Furthermore, by equating the coefficients of the terms $1, z, \cdots, z^\ell$ in (17), it follows that the coefficients of the polynomial $P_\ell(z)$ are given by

$$\begin{aligned} \mu_0 &= c_0, \\ \mu_1 &= c_1 + \nu_1 c_0, \\ \mu_2 &= c_2 + \nu_1 c_1 + \nu_2 c_0, \\ &\vdots \\ \mu_\ell &= c_\ell + \sum_{i=1}^{\min(\ell,m)} \nu_i c_{\ell-i}. \end{aligned} \tag{20}$$

However, the Padé rational approximant under the form $f_\tau^{[\ell/m]}(z) = P_\ell(z)/Q_m(z)$ is not the most useful for our purpose, since we will eventually deal with operators of order $2m$ related to the polynomial Q_m in the *pseudodifferential* framework. The following decomposition, which is more appropriate

for numerical implementation, can be easily derived from the previous one

$$f_\tau^{[\ell/m]}(z) = \frac{P_\ell(z)}{Q_m(z)} = \widehat{r}_0^{[\ell/m]}(z) + \sum_{j=1}^{m} \frac{\widehat{r}_j^{[\ell/m]}}{z - \widehat{q}_j^{[\ell/m]}}, \tag{21}$$

where $\{\widehat{q}_j^{[\ell/m]} : j = 1, \cdots, m\}$ are the zeros of $Q_m(z)$ and $\{\widehat{r}_j^{[\ell/m]} : j = 0, \cdots, m\}$ are given from the zeros of $P_\ell(z)$ and $Q_m(z)$. Let us precise that $\widehat{r}_0^{[\ell/m]}(z)$ is a polynomial of degree $\ell - m$ when $\ell > m$, otherwise this is a nonzero (respectively zero) constant when $\ell = m$ (respectively $\ell < m$).

The Padé approximants of the function $f_\tau(z)$ presented above are only valid for the real case, i.e., in the region $\{z > -1\}$ but are inaccurate for the branch-cut $\{z < -1\}$. Indeed, $f_\tau(z)$ becomes complex-valued whereas the Padé approximant $f_\tau^{[\ell/m]}(z)$ is a real number. In order to solve this problem we follow [31] and change the principal determination of the function by applying a rotation of the branch-cut with an angle θ. In our case, for $\tau = -\frac{1}{2}$, we write

$$\begin{aligned} f_{-\frac{1}{2}}(z) = \frac{1}{\sqrt{1+z}} &= \frac{1}{e^{\imath\frac{\theta}{2}}\sqrt{e^{-\imath\theta}(1+z)}} = \frac{e^{-\imath\frac{\theta}{2}}}{\sqrt{1+[e^{-\imath\theta}(1+z)-1]}} \\ &\simeq e^{-\imath\frac{\theta}{2}} f_{-\frac{1}{2}}^{[\ell/m]}\left(e^{-\imath\theta}(1+z)-1\right) = r_0^{[\ell/m]}(z) + \sum_{j=1}^{m} \frac{r_j^{[\ell/m]}}{z - q_j^{[\ell/m]}}, \end{aligned} \tag{22}$$

where $r_0^{[\ell/m]}(z) = e^{-\imath\frac{\theta}{2}}\widehat{r}_0^{[\ell/m]}(z)$, $r_j^{[\ell/m]} = e^{\imath\frac{\theta}{2}}\widehat{r}_j^{[\ell/m]}$ and $q_j^{[\ell/m]} = e^{\imath\theta}(\widehat{q}_j^{[\ell/m]} + 1) - 1$, for $j = 1, \cdots, m$.

4.3. **Implicit localization of HSLP *via* Padé approximants.** We can now write a local approximation of the nonlocal operator $\mathcal{P}$. The *exact inverse* of $\mathcal{H}$ can then be represented by the approximate principal symbol

$$\begin{aligned} \sigma_{[\mathcal{H}^{-1}]} &= \sigma_{[\mathcal{P}^2]} \\ &= -\frac{1}{k^2}\frac{1}{(1+z)} \\ &\simeq -\frac{1}{k^2}\left[r_0^{[\ell'/m']}(z) + \sum_{j=1}^{m'} \frac{r_j^{[\ell'/m']}}{z - q_j^{[\ell'/m']}}\right]\left[r_0^{[\ell''/m'']}(z) + \sum_{j=1}^{m''} \frac{r_j^{[\ell''/m'']}}{z - q_j^{[\ell''/m'']}}\right], \end{aligned} \tag{23}$$

with $z = -|\boldsymbol{\xi}|^2/k^2 \in \mathbb{R}^-$, when using the complex Padé rational approximants of order $[\ell'/m']$ and $[\ell''/m'']$ with a θ-rotation of the branch-cut. Since $\mathcal{P}^2$ is a pseudodifferential operator of order -2 as explained in Section 4.1, *so must be its symbol*, and the Padé orders must satisfy the following condition: $\ell' + \ell'' + 1 = m' + m''$. For this purpose, we split the symmetric formulation of the last equation of (23) into di-symmetrical factors, in terms of the Padé appproximation order, *to provide a symbol of global order* -2. Let us introduce the pseudodifferential operators $\widetilde{\mathcal{P}}_1$ and $\widetilde{\mathcal{P}}_2$ such that their symbols are

$$\begin{aligned} \sigma_{[\widetilde{\mathcal{P}}_1]} = \frac{1}{\imath k} f_{-\frac{1}{2}}^{[\ell_1-1/\ell_1]}(z) &= \frac{1}{\imath k} e^{-\imath\frac{\theta}{2}} f_{-\frac{1}{2}}^{[\ell_1-1/\ell_1]}\left(e^{-\imath\theta}(1+z)-1\right) \\ &= \frac{1}{\imath k}\left[\sum_{j=1}^{\ell_1} \frac{r_j^{[\ell_1-1/\ell_1]}}{z - q_j^{[\ell_1-1/\ell_1]}}\right] \end{aligned} \tag{24}$$

since $r_0^{[\ell_1-1/\ell_1]}=0$, and

$$\sigma_{[\widetilde{\mathcal{P}}_2]}=\frac{1}{\imath k}f_{-\frac{1}{2}}^{[\ell_2/\ell_2]}(z)=\frac{1}{\imath k}e^{-\imath\frac{\theta}{2}}f_{-\frac{1}{2}}^{[\ell_2/\ell_2]}\left(e^{-\imath\theta}(1+z)-1\right)$$
$$=\frac{1}{\imath k}\left[r_0^{[\ell_2/\ell_2]}+\sum_{j=1}^{\ell_2}\frac{r_j^{[\ell_2/\ell_2]}}{z-q_j^{[\ell_2/\ell_2]}}\right]. \tag{25}$$

Then the *exact inverse* of $\mathcal{H}$ is approximated by $\mathcal{H}^{-1}\simeq\widetilde{\mathcal{P}}_1\widetilde{\mathcal{P}}_2$ and its principal symbol reads

$$\begin{aligned}\sigma_{[\mathcal{H}^{-1}]} &\simeq \sigma_{[\widetilde{\mathcal{P}}_1\widetilde{\mathcal{P}}_2]}\\ &= -\frac{1}{k^2}\left[\sum_{j=1}^{\ell_1}\frac{r_j^{[\ell_1-1/\ell_1]}}{z-q_j^{[\ell_1-1/\ell_1]}}\right]\left[r_0^{[\ell_2/\ell_2]}+\sum_{j=1}^{\ell_2}\frac{r_j^{[\ell_2/\ell_2]}}{z-q_j^{[\ell_2/\ell_2]}}\right].\end{aligned} \tag{26}$$

By construction, the operator $\widetilde{\mathcal{P}}_1\widetilde{\mathcal{P}}_2$ is of order -2 and then the product $\widetilde{\mathcal{P}}_1\widetilde{\mathcal{P}}_2\mathcal{H}$ is a perturbation of the identity operator which is an important property for fast convergence of Krylov solvers. Indeed, it results in mesh refinement independent convergence because of eigenvalue clustering in the elliptic zone **E**. Moreover, from our construction by using appropriate Padé approximants well-adapted to the approximation in the hyperbolic zone **H**, the convergence will be weakly frequency dependent. This approximation will be denoted by GSLP$[\ell_1|\ell_2|\theta]$. Let us remark that the symbol of the preconditioned operator $\widetilde{\mathcal{P}}_1\widetilde{\mathcal{P}}_2\mathcal{H}$ with GSLP$[1|0|\theta]$ reads

$$\sigma_{[\widetilde{\mathcal{P}}_1\widetilde{\mathcal{P}}_2\mathcal{H}]}=2e^{\imath\frac{\theta}{2}}\frac{1+z}{(1-e^{\imath\theta})+z}. \tag{27}$$

Since $2e^{\imath\frac{\theta}{2}}$ is a constant term, GSLP$[1|0|\theta]$ is exactly the same as SLP given in (7) with $\alpha=1-e^{\imath\theta}$. For example, for $\theta=\pi/2$, we find $\alpha=1+\imath$. The class of GSLP$[\ell_1|\ell_2|\theta]$ preconditioners thus constitutes a high-order generalization of the standard Shifted Laplace Preconditioners.

REMARK.

In the GSLP context, one could imagine other preconditioners by using localized square-root operators. For example, one could consider an approximation of the non local operator $\mathcal{Q}$ of order 1 given by

$$\mathcal{Q}:=\mathcal{H}^{\frac{1}{2}}=[-\Delta-k^2]^{\frac{1}{2}} \tag{28}$$

with symbol

$$\sigma_{[\mathcal{Q}]}=\left(|\boldsymbol{\xi}|^2-k^2\right)^{\frac{1}{2}}=\imath k(1+z)^{\frac{1}{2}},\ z=-\frac{|\boldsymbol{\xi}|^2}{k^2}\in\mathbb{R}^-. \tag{29}$$

To localize $\mathcal{Q}$, the Padé representation can be used with $\tau=\frac{1}{2}$ instead of $\tau=-\frac{1}{2}$. Then to obtain a preconditioner, the rational approximation of $\mathcal{H}=\mathcal{Q}^2$ must be inverted. However, after discretization by the FEM, this would lead to the numerical solution of a very large linear system of coupled damped Helmholtz equations. This direction which is too computationally expensive has therefore been abandoned.

4.4. **GSLP: algebraic formulation.** In the previous section we have presented a class of rational approximations of $\mathcal{H}^{-1}$ through symbolic calculus within the *pseudodifferential operator framework*. In this section we present the effective construction of GSLP as a kind of *hybrid preconditioner*, using the representation of $\mathcal{H}^{-1}$ to compute $[\mathbb{H}_h]^{-1}$ in the FEM context. By *hybrid*, we mean that we combine both the continuous operator approach *via* variational formulations, and discrete methods including FEM and standard algebraic preconditioners. Working at the weak formulation level allows to naturally handle boundary conditions in the formulations.

Let us come back to the Helmholtz matrix that writes, in the FEM context

$$[\mathbb{H}_h] = [\mathbb{S}_h] - k^2[\mathbb{M}_h] - \imath k[\mathbb{B}_h].$$

Setting $[\widetilde{\mathbb{S}}_h] = [\mathbb{S}_h] - \imath k[\mathbb{B}_h]$ and if $[\mathbb{I}]$ denotes the identity matrix, it follows that

$$\begin{aligned}[\mathbb{H}_h] &= [\widetilde{\mathbb{S}}_h] - k^2[\mathbb{M}_h] \\ &= -k^2[\mathbb{M}_h]\left([\mathbb{I}] - \frac{1}{k^2}[\mathbb{M}_h]^{-1}[\widetilde{\mathbb{S}}_h]\right).\end{aligned}$$

Therefore, the inverse of $[\mathbb{H}_h]$ writes

$$[\mathbb{H}_h]^{-1} = -\frac{1}{k^2}\left([\mathbb{I}] - \frac{1}{k^2}[\mathbb{M}_h]^{-1}[\widetilde{\mathbb{S}}_h]\right)^{-1}[\mathbb{M}_h]^{-1}.$$

The matrix term $\left([\mathbb{I}] - \frac{1}{k^2}[\mathbb{M}_h]^{-1}[\widetilde{\mathbb{S}}_h]\right)^{-1}$ is evaluated by using pseudo-representation of $(1+z)^{-1}$ given in (26). In contrast to the continuous case, the discrete approach naturally includes the boundary condition on Γ^∞. Then, by rearranging the terms, we find

$$[\mathbb{H}_h]^{-1} \simeq \mathbb{P}_1\mathbb{P}_2 \tag{30}$$

where $\mathbb{P}_1$ and $\mathbb{P}_2$ are given by

$$\mathbb{P}_1 := \left[\sum_{j=1}^{\ell_1} r_j^{[\ell_1-1/\ell_1]}\left([\widetilde{\mathbb{S}}_h] + q_j^{[\ell_1-1/\ell_1]}k^2[\mathbb{M}_h]\right)^{-1}\right] \tag{31}$$

and

$$\mathbb{P}_2 := \left[r_0^{[\ell_2/\ell_2]}[\mathbb{I}] - k^2[\mathbb{M}_h]\sum_{j=1}^{\ell_2} r_j^{[\ell_2/\ell_2]}\left([\widetilde{\mathbb{S}}_h] + q_j^{[\ell_2/\ell_2]}k^2[\mathbb{M}_h]\right)^{-1}\right] \tag{32}$$

The Helmholtz matrix is then preconditioned as follows

$$\mathbb{P}_1\mathbb{P}_2[\mathbb{H}_h] \tag{33}$$

As one can see, the matrices

$$\left([\widetilde{\mathbb{S}}_h] + q_j^{[\ell_1-1/\ell_1]}k^2[\mathbb{M}_h]\right) = \left([\mathbb{S}_h] + q_j^{[\ell_1-1/\ell_1]}k^2[\mathbb{M}_h] - \imath k[\mathbb{B}_h]\right), \tag{34}$$

$$\left([\widetilde{\mathbb{S}}_h] + q_j^{[\ell_2/\ell_2]}k^2[\mathbb{M}_h]\right) = \left([\mathbb{S}_h] + q_j^{[\ell_2/\ell_2]}k^2[\mathbb{M}_h] - \imath k[\mathbb{B}_h]\right) \tag{35}$$

involved in (31) and (32) correspond to discrete shifted Laplace operators. They have the same sparsity pattern as the Helmholtz matrix $[\mathbb{H}_h]$ and the discrete shifted Laplace operator $[\mathbb{A}_{(\alpha),h}]$. They can be "inverted" efficiently by using sparse ILUT or multigrid methods since the related linear systems are defined by damped Helmholtz operators. Furthermore, iteratively solving the Helmholtz system (5) preconditioned by GSLP$[\ell_1|\ell_2|\theta]$ as follows

$$\mathbb{P}_1\mathbb{P}_2\left([\mathbb{H}_h]\mathbf{u}_h = \mathbf{b}_h\right) \tag{36}$$

requires for each iteration the usual Matrix-Vector Product (MVP) with $[\mathbb{H}_h]$, plus $(\ell_1 + \ell_2)$ LU/ILU-solutions for applying the preconditioner (rather than just one for the classic SLP). However, one crucial point is that these ℓ_1 and ℓ_2 linear systems can be *solved in parallel* since they are involved in the preconditioner definition (31)-(32) through *summation*. Therefore, the application of HSLP can be seen as two times more costly than SLP for one iteration. Let $\mathbb{F}_{1j}$ and $\mathbb{F}_{2j}$ represent the LU/ILU factorization of the matrices in (34) and (35) respectively. Then the procedure for computing $\mathbf{y} = \mathbb{P}_1\mathbb{P}_2\mathbf{x}$ is directly given by Algorithm 1.

Algorithm 1: GSLP operation $\mathbf{y} = \mathbb{P}_1\mathbb{P}_2\mathbf{x}$.

$\mathbf{x}_{\text{temp}} = 0$;
for $j = 1 : \ell_2$ **do**
  $\mathbf{x}_{\text{temp}} \longleftarrow \mathbf{x}_{\text{temp}} + r_j^{[\ell_2/\ell_2]}[\mathbb{F}_{2j}]^{-1}\mathbf{x}$
$\mathbf{x}_{\text{temp}} \longleftarrow r_0^{[\ell_2/\ell_2]}\mathbf{x} - k^2[\mathbb{M}_h]\mathbf{x}_{\text{temp}}$;
$\mathbf{y} = 0$;
for $j = 1 : \ell_1$ **do**
  $\mathbf{y} \longleftarrow \mathbf{y} + r_j^{[\ell_1-1/\ell_1]}[\mathbb{F}_{1j}]^{-1}\mathbf{x}_{\text{temp}}$;

4.5. **Numerical study of the eigenvalues clustering.** In order to analyze the eigenvalue distribution of the discrete Helmholtz operator preconditioned by HSLP as written in (33), let us reconsider the 1D scattering problem introduced in Subsection 3.2 for the SLP clustering illustration.

Figure 2 shows the eigenvalues representation of the Helmholtz matrix preconditioned by HSLP. We represent likewise the continuous eigenvalues of the preconditioned Helmholtz operator given by

$$\sigma_{[\widetilde{\mathcal{P}}_1\widetilde{\mathcal{P}}_2\mathcal{H}]} = \left[\sum_{j=1}^{\ell} \frac{r_j^{[\ell-1/\ell]}}{z - q_j^{[\ell-1/\ell]}}\right](1+z)\left[r_0^{[\ell/\ell]} + \sum_{j=1}^{\ell} \frac{r_j^{[\ell/\ell]}}{z - q_j^{[\ell/\ell]}}\right]. \tag{37}$$

We use the Padé approximation GSLP$[1|0|\frac{\pi}{2}]$ in Figure 2(a). This is the lowest order in the HSLP context. Furthermore, as said above, this represents the SLP case with $\alpha = 1 + \imath$. Figures 2(b), 2(c), 2(d), 2(e), 2(f) report the GSLP$[\ell|\ell|\frac{\pi}{2}]$ approximation in the "continuous" (37) and "algebraic" (33) context for

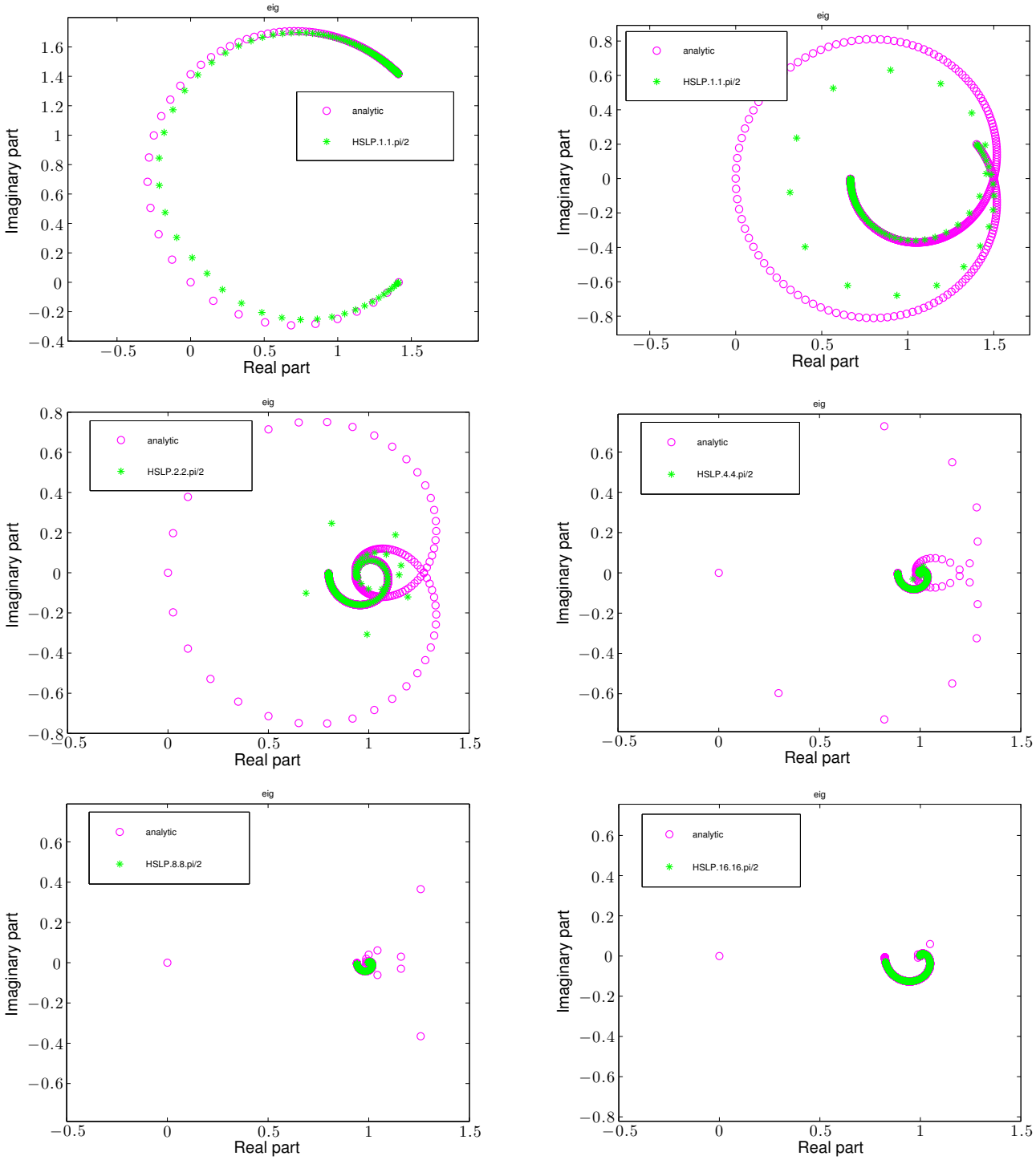

FIGURE 2. GSLP$[\ell|\ell|\frac{\pi}{2}]$ eigenvalues clustering for the 1D scattering problem ($k = 20\pi$, $n_\lambda = 80$).

$\ell = 1, 2, 4, 8, 16$ respectively. Note that from numerical studies it appears that $\theta = \pi/2$ provides the most accurate results concerning the Padé approximation. We will keep this value all along the paper, even for the more complex situations studied in Section 5.

GSLP$[\ell|\ell|\frac{\pi}{2}]$ clearly leads to an improved clustering of the eigenvalues, which is due in particular to a better approximation of the propagative (zone $\mathbf{H}$) and evanescent (zone $\mathbf{E}$) modes. Furthermore, the grazing modes (zone $\mathbf{G}$) are also well approximated: for a given discretization, the modes of the zone $\mathbf{G}$ are progressively pushed towards the endpoint $(1,0)$ as the order of the Padé approximation is increased. Only a single "continuous" eigenvalue remains close to zero, which represents the situation where $|\boldsymbol{\xi}| = k$. This can be interpreted as $z = -1$ in (37) implying that we are close to a resonance. This situation does not arise in the discrete context, since the dissipative Helmholtz operator with Dirichlet boundary condition and absorbing boundary condition leads to a well-posed problem. This implies that eigenvalues are rolled and clustered around the endpoint $(1,0)$ when we increase the order ℓ. Therefore, this will result in fast convergence of an iterative solver since we are solving a preconditioned equation given by a small compact perturbation of the identity operator.

5. Numerical Examples

In this section we present numerical simulations for testing the convergence acceleration of Krylov-type iterative solvers preconditioned with GSLP. Comparisons will be made with the classic SLP method, taking the "optimal" parameter $\alpha = 1 + \frac{1}{2}\imath$. We consider the scattering of an incident acoustic plane wave $u^{\text{inc}} = e^{-\imath k x_1}$ coming from $+\infty$. The computational region is meshed with a discretization density of $n_\lambda = \lambda/h$ gridpoints per wavelength. We use Gmsh/GetDP [24,25] to generate meshes and matrix terms involved in linear system (5). The SLP and GSLP algorithms are implemented in Matlab. Linear systems are solved iteratively by GMRES, unrestarted by default. The convergence criterion is set to 10^{-9}. In the case of restarted GMRES (GMRES(m)), the Krylov subspace dimension is set to $m = 50$.

5.1. **Two-dimensional examples.**

This subsection presents numerical results obtained on three different geometrical configurations in 2D, in order to illustrate the robustness and efficiency of GSLP$[\ell|\ell|\frac{\pi}{2}]$, with $\ell = 1, 2, 4, 8, 16$.

5.1.1. *Scattering by the unit disc.*

We consider the scattering by the unit disc $\Omega^- = \{|\mathbf{x}| < 1\}$. The boundary Γ is the circle $\{|\mathbf{x}| = R = 1\}$ and the fictitious boundary Γ^∞ is set to $\{|\mathbf{x}| = R^\infty = 2\}$.

Influence of the wavenumber. We report in Figure 3 the number of unrestarted GMRES iterations with respect to the wavenumber k. The discretization density is set to $n_\lambda = 10$. In a first step, for purely theoretical purposes, we use an exact LU to invert SLP ($\mathbb{A}^{\imath\sqrt{\alpha}k}_{(\alpha),h}$) and HSLP (matrix terms involved in (31) and (32)). Then ILUT(ε) is used to solve the preconditioners. We decrease the fill-in of the L/U factors progressively by increasing the ILU threshold: $\varepsilon = 10^{-5}, 10^{-4}, 10^{-3}$. A linear increase of the number of iterations with respect to the wavenumber is observed for SLP and GSLP$[1|1|\frac{\pi}{2}]$, while a weak dependency is observed for GSLP$[2|2|\frac{\pi}{2}]$. When $\ell \geq 4$, GSLP$[\ell|\ell|\frac{\pi}{2}]$ provides convergence quasi

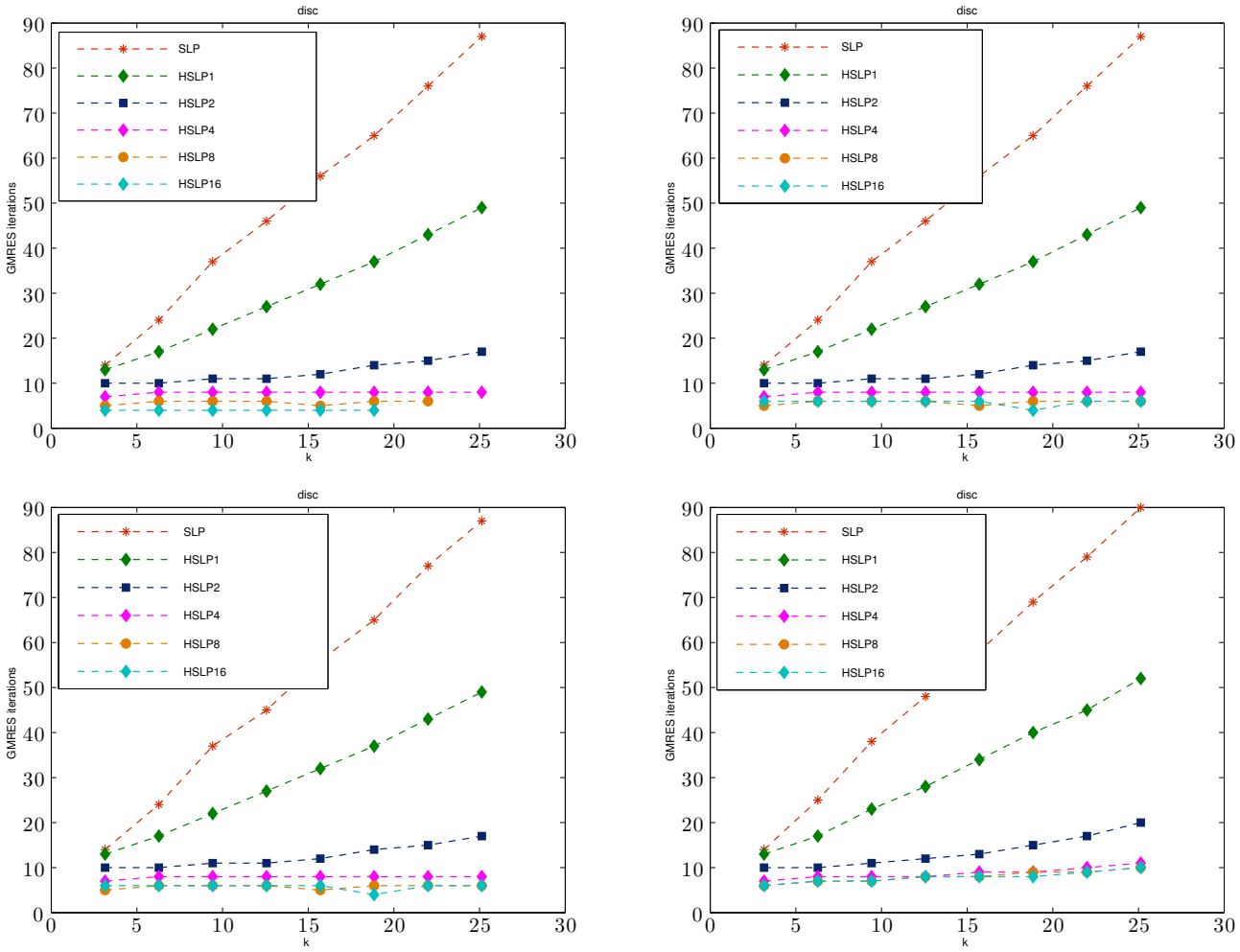

FIGURE 3. Scattering by a unit disc: influence of the wavenumber with $n_\lambda = 10$.

independent from the wavenumber, which is in accordance with the eigenvalue clustering observed in Subsection 4.5.

Influence of the discretization density. Figure 4 reports the number of unrestarted GMRES iterations with respect to the discretization density n_λ for the wavenumber $k = 2\pi$, using likewise an exact LU and ILUT(ε), with $\varepsilon = 10^{-5}, 10^{-4}, 10^{-3}$.

A convergence quasi-independent of the mesh size can be observed for both SLP and GSLP when using an exact LU (Figure 4.a) or sufficiently accurate ILUT(ε) (Figures 4.b, 4.c). However, a dependency to n_λ appears when using a poor ILUT(ε) (Figure 4.d).

Computational cost. In order to analyze the computational cost of HSLP, in addition to the number of GMRES iterations reported above, we need to analyze the ILUT fill-in. Coming back to the algebraic formulation of GSLP presented in Subsection 4.4, application of GSLP requires the ILUT-inversion of the matrix terms

$$\left([\mathbb{S}_h] + q_j^{[\ell_1 - 1/\ell_1]} k^2 [\mathbb{M}_h] - \imath k [\mathbb{B}_h]\right) \text{ and } \left([\mathbb{S}_h] + q_j^{[\ell_2/\ell_2]} k^2 [\mathbb{M}_h] - \imath k [\mathbb{B}_h]\right),$$

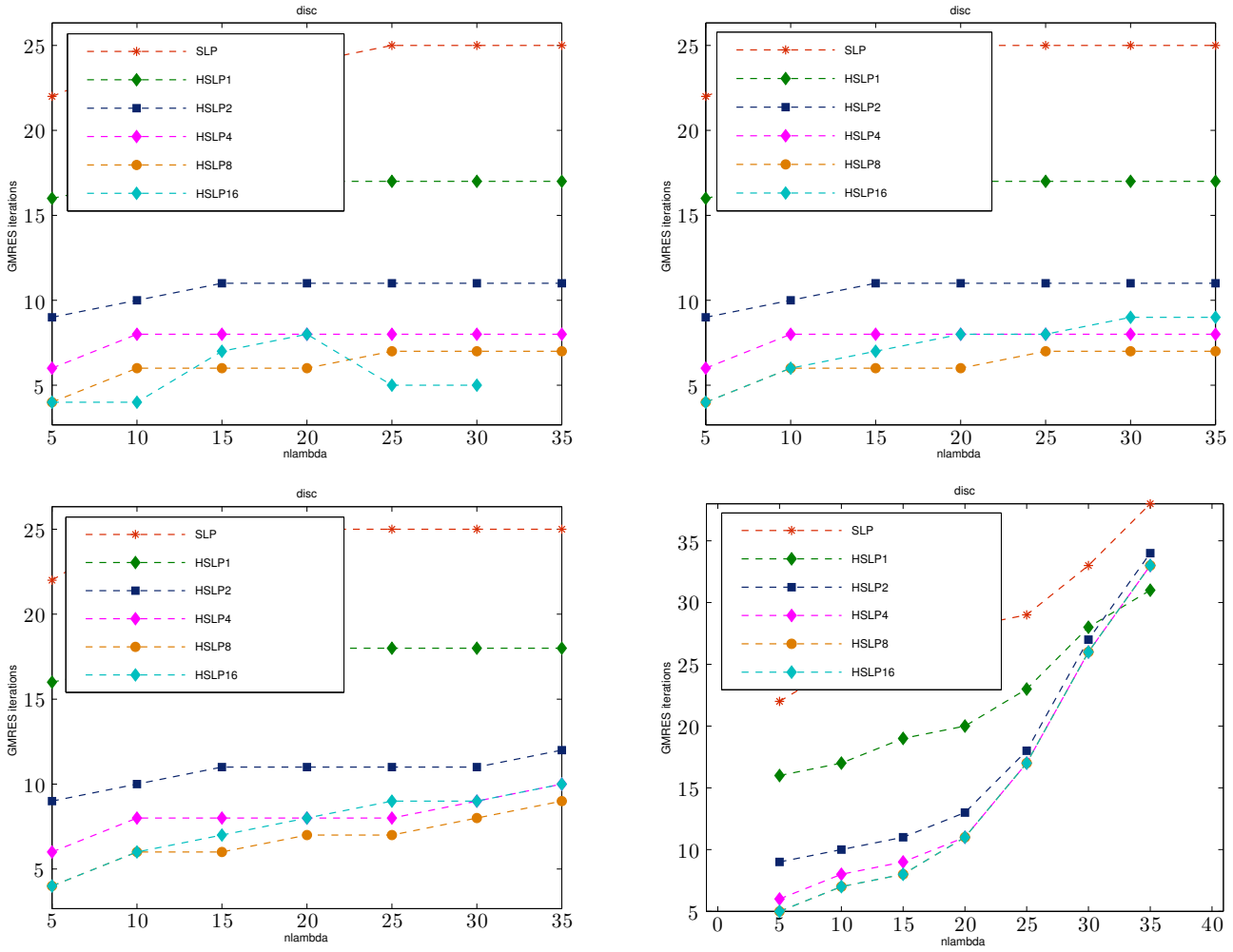

FIGURE 4. Scattering by a unit disc: influence of the discretization density for $k = 2\pi$.

which are similar to the SLP discrete operator $\mathbb{A}^{ik}_{(\alpha),h}$ with $\alpha = -q_j^{[\ell_1-1/\ell_1]}$ or $-q_j^{[\ell_2/\ell_2]}$. When the Padé complex shifts have large enough imaginary parts, the ILUT(ε) factorization exhibits more stability and for a given drop tolerance ε, the fill-in of the L/U factors remains very low [33]. Otherwise, the factorization may be unstable, the fill-in becomes too much exuberant and then, the preconditioner useless.

For example, for $k = 2\pi$, $n_\lambda = 35$, the exact LU factorization of the Helmholtz matrix (whose number of nonzeros entries is 90688) has a number of nonzeros entries $\texttt{nnz}(\mathrm{L}) = 23668407$. Tables 1 and 2 present the number of fill-in coefficients $\texttt{nnz}(\mathrm{L})$ of the ILUT factorizations for two different threshold values ($\varepsilon = 10^{-3}$ and $\varepsilon = 10^{-4}$), for all the coefficients $q_j^{[\ell-1,\ell]}$ and $q_j^{[\ell,\ell]}$ in the Padé expansions with $\ell = 4$ and $\ell = 8$. As expected [33], more coefficients are needed when the imaginary part of the q_j coefficient becomes smaller. However, the number of non-zero entries always remains much smaller than for a complete LU factorization: from 1% ($\texttt{nnz}(\mathrm{L})$=216177) to 1.5% ($\texttt{nnz}(\mathrm{L})$=379974) in the worst case (i.e. for the shift with the smallest imaginary part) for ILUT thresholds $\varepsilon = 10^{-3}$ and $\varepsilon = 10^{-4}$, respectively.

Furthermore, SLP leads to $\texttt{nnz}(\mathrm{L})$=209752 and $\texttt{nnz}(\mathrm{L})$=361305 for the same ILUT thresholds, i.e., about the same amount of fill-in.

TABLE 1. Scattering by a unit disc: $\texttt{nnz}(\mathrm{L})$ of ILUT(ε) with $\ell = 4$, for $k = 2\pi$ and $n_\lambda = 35$.

$q_j^{[3/4]}$	$\varepsilon = 10^{-3}$	$\varepsilon = 10^{-4}$	$q_j^{[4/4]}$	$\varepsilon = 10^{-3}$	$\varepsilon = 10^{-4}$
$q_1^{[3/4]} = -1 - 25.27\imath$	174380	265587	$q_1^{[4/4]} = -1 - 7.548\imath$	190673	303043
$q_2^{[3/4]} = -1 - 2.239\imath$	201517	333875	$q_2^{[4/4]} = -1 - 1.420\imath$	204501	343899
$q_3^{[3/4]} = -1 - 0.446\imath$	210286	362579	$q_3^{[4/4]} = -1 - 0.333\imath$	211497	365934
$q_4^{[3/4]} = -1 - 0.039\imath$	215901	378274	$q_4^{[4/4]} = -1 - 0.031\imath$	216177	378657

TABLE 2. Scattering by a unit disc: $\texttt{nnz}(\mathrm{L})$ of ILUT(ε) with $\ell = 8$, for $k = 2\pi$ and $n_\lambda = 35$.

$q_j^{[7/8]}$	$\varepsilon = 10^{-3}$	$\varepsilon = 10^{-4}$	$q_j^{[8/8]}$	$\varepsilon = 10^{-3}$	$\varepsilon = 10^{-4}$
$q_1^{[7/8]} = -1 - 103.0\imath$	150336	218619	$q_1^{[8/8]} = -1 - 28.61\imath$	172276	261511
$q_2^{[7/8]} = -1 - 10.86\imath$	186316	292173	$q_2^{[8/8]} = -1 - 6.663\imath$	191973	306387
$q_3^{[7/8]} = -1 - 3.500\imath$	197845	323207	$q_3^{[8/8]} = -1 - 2.608\imath$	200401	330447
$q_4^{[7/8]} = -1 - 1.484\imath$	204241	342867	$q_4^{[8/8]} = -1 - 1.203\imath$	205445	347067
$q_5^{[7/8]} = -1 - 0.673\imath$	208365	357191	$q_5^{[8/8]} = -1 - 0.570\imath$	209237	359363
$q_6^{[7/8]} = -1 - 0.285\imath$	212153	367646	$q_6^{[8/8]} = -1 - 0.247\imath$	212549	368955
$q_7^{[7/8]} = -1 - 0.092\imath$	214853	376217	$q_7^{[8/8]} = -1 - 0.080\imath$	215102	376783
$q_8^{[7/8]} = -1 - 0.009\imath$	216882	379936	$q_8^{[8/8]} = -1 - 0.008\imath$	216899	379974

Since all the incomplete factorizations in GSLP can be performed concurrently, this means that, if implemented in parallel, the user-facing factorization time of GSLP is comparable to that of SLP. In addition, more stable and robust incomplete factorizations [33], multigrid methods [19] or other approximation methods could also be used. In particular, the threshold should be adapted depending on the magnitude of the imaginary part of the q_j like in [33] for sparsifying the factorizations while being more robust. With such improvements and a parallel implementation we can thus expect that, even on this simple example where SLP is already quite effective, GSLP would still outperform it, especially at high frequencies. These numerical studies are the subject of current investigations and are beyond the scope of the present paper.

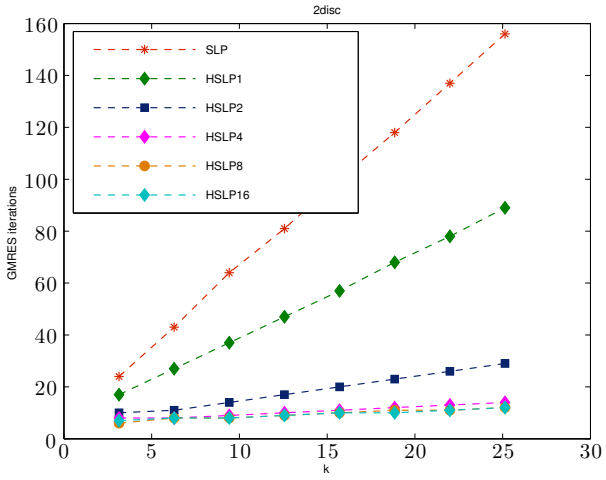

FIGURE 5. Scattering by two unit discs: influence of the wavenumber for $n_\lambda = 10$, with ILUT(10^{-3}).

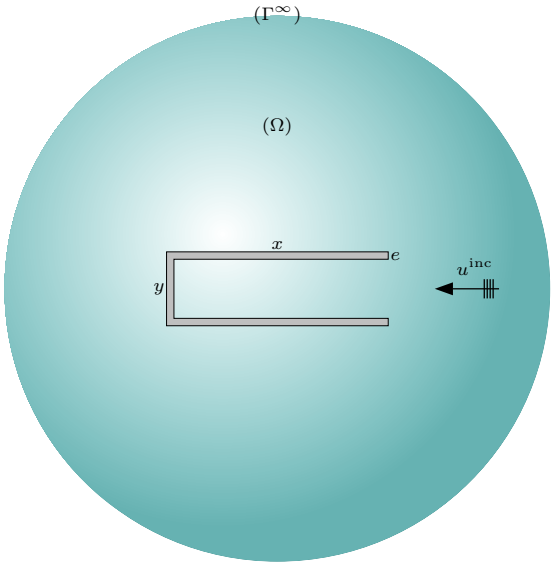

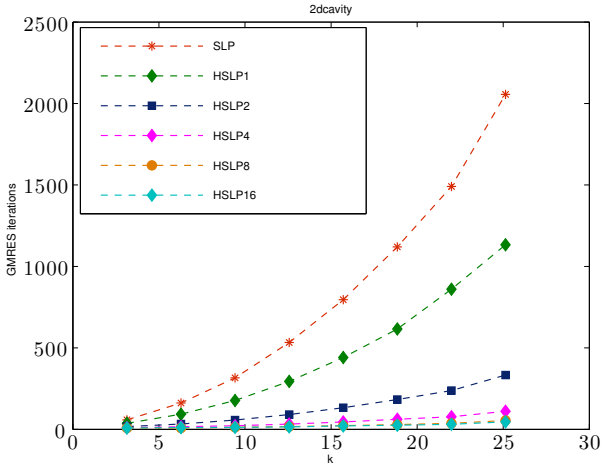

FIGURE 6. Scattering by a 2D open cavity: influence of the wavenumber for $n_\lambda = 10$, with ILUT(10^{-3})

5.1.2. *Scattering by two unit discs.* We consider the scattering by two unit discs $\Omega^- = \{|\mathbf{x} + (0, 1.375)| < 1\} \cup \{|\mathbf{x} - (0, 1.375)| < 1\}$. The fictitious boundary Γ^∞ is set to $\{|\mathbf{x}| = R^\infty = 3.5\}$.

Figure 5 reports the unrestarted GMRES iterations with respect to the wavenumber, using ILUT(10^{-3}). A linear dependence with respect to k can be observed for SLP. GSLP leads to a convergence weakly dependent of k provided the order ℓ is large enough. Satisfactory convergence is already achieved for $\ell = 2$.

5.1.3. *Scattering by an open cavity.* The scatterer Ω^- is an elongated rectangular cavity with dimensions: $y = 1$, $x = 3$ and $e = 1/10$. The fictitious boundary Γ^∞ is the circle of radius $R^\infty = 3$. The geometry and the computational domain are represented in Figure 6.

We report in Figure 6 the unrestarted GMRES iterations with respect to the wavenumber, with ILUT(10^{-3}). SLP requires a huge number of iterations even for moderate wavenumbers. GSLP clearly improves the convergence rate as ℓ is increased. Furthermore we repeat the experience above using a restarted GMRES ($m = 50$). The results are reported in Table 3. In this case, SLP fails to converge for $k \geq 3\pi$, and GSLP achieves very fast convergence for $\ell \geq 8$. The same simulations are reported in Table 4 for ILUT(10^{-4}). We can again see the robustness and efficiency of GSLP, most particularly for $\ell = 8$.

TABLE 3. Scattering by a 2D open cavity using ILUT(10^{-3}): Number of iterations vs. k with GMRES(50), for $n_\lambda = 10$.

k	π	2π	3π	4π	5π	6π	7π	8π
SLP	73	1281	–	7505	–	–	–	–
GSLP[1|1|$\frac{\pi}{2}$]	37	329	833	2127	4191	–	–	–
GSLP[2|2|$\frac{\pi}{2}$]	17	33	70	316	507	25395	2108	–
GSLP[4|4|$\frac{\pi}{2}$]	10	16	22	32	45	105	256	–
GSLP[8|8|$\frac{\pi}{2}$]	8	11	12	17	23	29	37	55
GSLP[16|16|$\frac{\pi}{2}$]	8	10	12	15	21	25	31	46

TABLE 4. Scattering by a 2D open cavity using ILUT(10^{-4}): number of iterations vs. k with GMRES(50), for $n_\lambda = 10$.

k	π	2π	3π	4π	5π	6π	7π	8π
SLP	74	1291	3790	5814	9227	–	–	–
GSLP[1|1|$\frac{\pi}{2}$]	37	310	795	2214	2880	24494	–	–
GSLP[2|2|$\frac{\pi}{2}$]	17	33	59	276	420	4313	1184	–
GSLP[4|4|$\frac{\pi}{2}$]	9	15	21	30	43	96	205	2444
GSLP[8|8|$\frac{\pi}{2}$]	6	9	11	13	18	22	28	40
GSLP[16|16|$\frac{\pi}{2}$]	6	7	8	9	10	13	15	24

Computational cost. To fix the ideas, let us consider GSLP[8|8|$\frac{\pi}{2}$] with $k = 8\pi$, $n_\lambda = 10$ and ILUT(10^{-3}). The resulting linear system has size $n_h = 50717$ and the exact LU factorization of the Helmholtz matrix has a number of nonzeros entries $\texttt{nnz}(\mathrm{L}) = 274562603$. We report in Tables 5 and 6 the fill-in for each Padé coefficient $q_j^{[\ell-1/\ell]}$ and $q_j^{[\ell/\ell]}$ for $\ell = 4, 8$, respectively.

TABLE 5. Scattering by a 2D open cavity: $\mathtt{nnz}(\mathrm{L})$ of ILUT(ε) for $\ell = 4$, with $k = 8\pi$ and $n_\lambda = 10$.

$q_j^{[3/4]}$	$\varepsilon = 10^{-3}$	$\varepsilon = 10^{-4}$	$q_j^{[4/4]}$	$\varepsilon = 10^{-3}$	$\varepsilon = 10^{-4}$
$q_1^{[3/4]} = -1 - 25.27\imath$	524106	762118	$q_1^{[4/4]} = -1 - 7.548\imath$	617451	923345
$q_2^{[3/4]} = -1 - 2.239\imath$	801945	1294507	$q_2^{[4/4]} = -1 - 1.420\imath$	902578	1514848
$q_3^{[3/4]} = -1 - 0.446\imath$	1351443	2553901	$q_3^{[4/4]} = -1 - 0.333\imath$	1547823	3012681
$q_4^{[3/4]} = -1 - 0.039\imath$	5240210	9171010	$q_4^{[4/4]} = -1 - 0.031\imath$	5828754	9434013

TABLE 6. Scattering by a 2D open cavity: $\mathtt{nnz}(\mathrm{L})$ of ILUT(ε) for $\ell = 8$, with $k = 8\pi$ and $n_\lambda = 10$.

$q_j^{[7/8]}$	$\varepsilon = 10^{-3}$	$\varepsilon = 10^{-4}$	$q_j^{[8/8]}$	$\varepsilon = 10^{-3}$	$\varepsilon = 10^{-4}$
$q_1^{[7/8]} = -1 - 103.0\imath$	500880	720980	$q_1^{[8/8]} = -1 - 28.61\imath$	519813	754164
$q_2^{[7/8]} = -1 - 10.86\imath$	579935	855805	$q_2^{[8/8]} = -1 - 6.663\imath$	631867	950881
$q_3^{[7/8]} = -1 - 3.500\imath$	722136	1129234	$q_3^{[8/8]} = -1 - 2.608\imath$	773114	1233590
$q_4^{[7/8]} = -1 - 1.484\imath$	891423	1490478	$q_4^{[8/8]} = -1 - 1.203\imath$	946518	1613353
$q_5^{[7/8]} = -1 - 0.673\imath$	1145139	2072055	$q_5^{[8/8]} = -1 - 0.570\imath$	1220364	2247075
$q_6^{[7/8]} = -1 - 0.285\imath$	1673515	3303074	$q_6^{[8/8]} = -1 - 0.247\imath$	1804374	3602307
$q_7^{[7/8]} = -1 - 0.092\imath$	3304421	6568973	$q_7^{[8/8]} = -1 - 0.080\imath$	3599188	6964951
$q_8^{[7/8]} = -1 - 0.009\imath$	6096331	9356284	$q_8^{[8/8]} = -1 - 0.008\imath$	6178105	9388780

One can clearly see that using ILUT(10^{-3}), the maximum fill-in for all the Padé coefficients is less than 3% of that of the Helmholtz matrix exact LU factorization. Since all of the ILUT can be computed in parallel as well as the preconditioning operation in the GMRES (as said above), the scalability of GSLP is very promising in this geometrically more complex case.

5.2. **Three-dimensional examples.** We consider the scattering by one ($\Omega^- = \{|\mathbf{x}| < 1\}$, $\Gamma^\infty = \{|\mathbf{x}| = R^\infty = 2\}$) or two ($\Omega^- = \{|\mathbf{x} + (0, 1.375, 0)| < 1\} \cup \{|\mathbf{x} - (0, 1.375, 0)| < 1\}$, $\Gamma^\infty = \{|\mathbf{x}| = R^\infty = 3.5\}$) unit spheres. We report in Figures 7 and 8 the convergence of unrestarted GMRES with ILUT(10^{-3}). In both cases, we consider $n_\lambda = 10$. It is clear that GSLP improves the convergence rate, most particularly when the frequency increases or/and when multiple scattering arises between the two spheres.

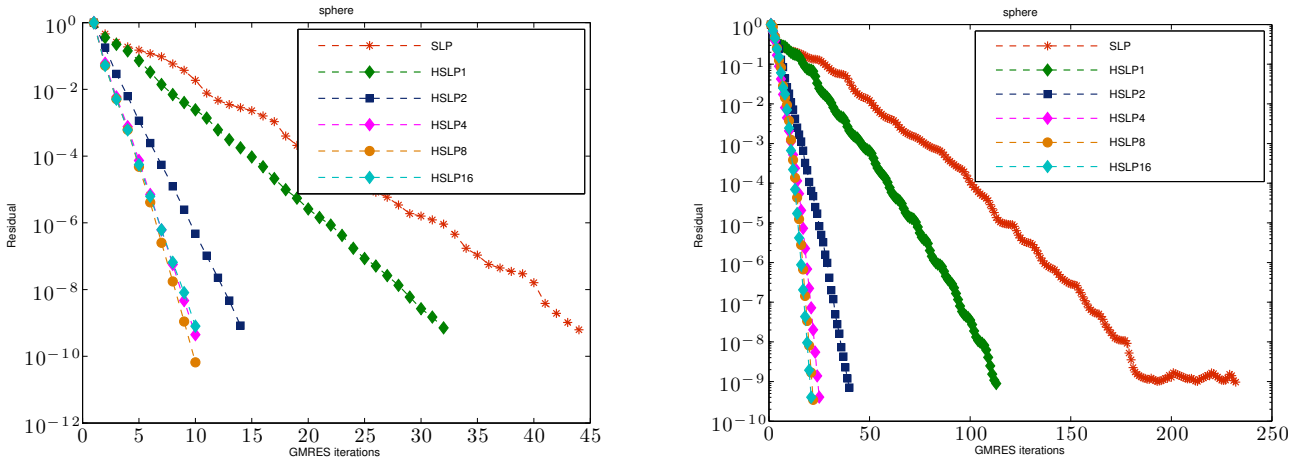

FIGURE 7. Scattering by the unit sphere for $n_\lambda = 10$, with ILUT(10^{-3}).

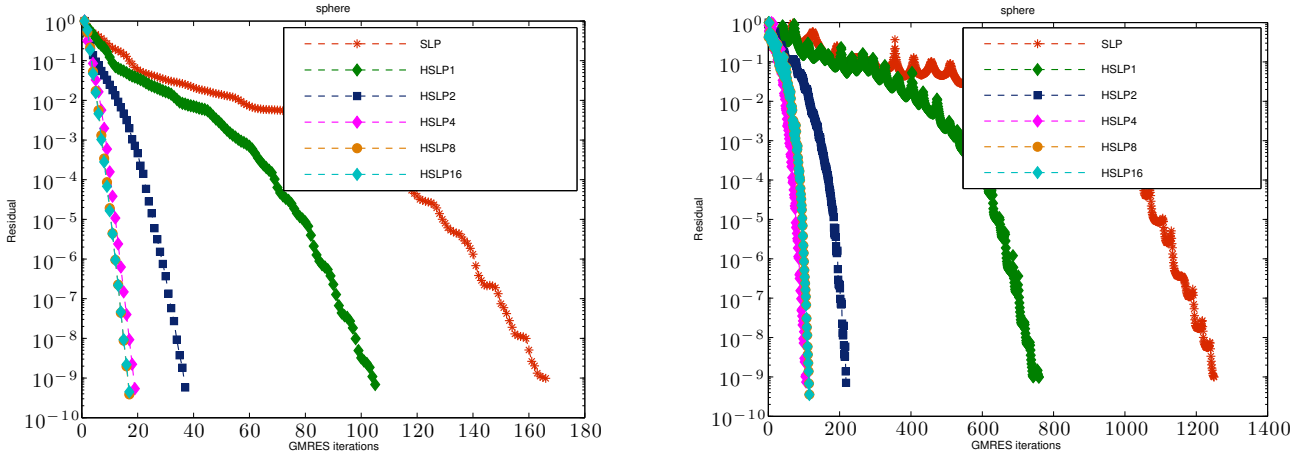

FIGURE 8. Scattering by two unit spheres for $n_\lambda = 10$, with ILUT(10^{-3}).

6. CONCLUSION

We have developped a new class of preconditioners for the Helmholtz equation. The method derives from an analytic approximation of the *inverse* of the Helmholtz operator by using Padé approximants. The resulting high-order method is an extension of the so-called Shifted Laplace preconditioning technique and has been shown through various 2D and 3D numerical examples to be robust and promising.

However the GSLP method is limited when the order increases because the imaginary parts of the shifting coeficients q_j become smaller. This remains an open problem for further investigations.

Acknowledgments. Ibrahim ZANGRÉ gratefully acknowledge support from the EADS foundation and the Agence Nationale pour la Recherche (http://microwave.math.cnrs.fr/) through grants [089-1009-1006] and [ANR-09-BLAN-0057-01] respectively.

Authors' Contributions. All authors have read and approved the final version of the manuscript. The authors contributed equally to this work.

Conflicts of Interest. The authors declare that there are no conflicts of interest regarding the publication of this paper.

References

[1] T. Airaksinen, A. Pennanen, J. Toivanen, A Damping Preconditioner for Time-Harmonic Wave Equations in Fluid and Elastic Material, J. Comput. Phys. 228 (2009), 1466–1479. https://doi.org/10.1016/j.jcp.2008.10.036.

[2] X. Antoine, H. Barucq, A. Bendali, Bayliss–Turkel–Like Radiation Conditions on Surfaces of Arbitrary Shape, J. Math. Anal. Appl. 229 (1999), 184–211. https://doi.org/10.1006/jmaa.1998.6153.

[3] X. Antoine, C. Geuzaine, K. Ramdani, Computational Methods for Multiple Scattering at High Frequency with Applications to Periodic Structure Calculations, in: Progress in Computational Physics (PiCP) Vol 1: Wave Propagation in Periodic Media, Bentham Science Publishers, 2010: pp. 73–107. https://doi.org/10.2174/978160805150211001010073.

[4] Y. Azulay, E. Treister, Multigrid-Augmented Deep Learning Preconditioners for the Helmholtz Equation, SIAM J. Sci. Comput. 45 (2022), S127–S151. https://doi.org/10.1137/21m1433514.

[5] G.A. Baker, P. Graves-Morris, Padé Approximants, 2nd ed., Cambridge University Press, Cambridge, 1996. https://doi.org/10.1017/CBO9780511530074.

[6] A. Bayliss, C.I. Goldstein, E. Turkel, An Iterative Method for the Helmholtz Equation, J. Comput. Phys. 49 (1983), 443–457. https://doi.org/10.1016/0021-9991(83)90139-0.

[7] M. Bollhöfer, M.J. Grote, O. Schenk, Algebraic Multilevel Preconditioner for the Helmholtz Equation in Heterogeneous Media, SIAM J. Sci. Comput. 31 (2009), 3781–3805. https://doi.org/10.1137/080725702.

[8] Y. Boubendir, A. Bendali, M.B. Fares, Coupling of a Non-overlapping Domain Decomposition Method for a Nodal Finite Element Method with a Boundary Element Method, Int. J. Numer. Methods Eng. 73 (2007), 1624–1650. https://doi.org/10.1002/nme.2136.

[9] C. Brezinski, History of Continued Fractions and Padé Approximants, Springer Berlin, 1991. https://doi.org/10.1007/978-3-642-58169-4.

[10] G. Chen, J. Zhou, Boundary Elements Methods, Academic Press, 1992.

[11] L. Demanet, L. Ying, Discrete Symbol Calculus, SIAM Rev. 53 (2011), 71–104. https://doi.org/10.1137/080731311.

[12] G.C. Diwan, M.S. Mohamed, Iterative Solution with Shifted Laplace Preconditioner for Plane Wave Enriched Isogeometric Analysis and Finite Element Discretization for High-Frequency Acoustics, Comput. Methods Appl. Mech. Eng. 384 (2021), 114006. https://doi.org/10.1016/j.cma.2021.114006.

[13] S. Duan, H. Wu, Adaptive FEM for Helmholtz Equation with Large Wavenumber, J. Sci. Comput. 94 (2022), 21. https://doi.org/10.1007/s10915-022-02074-5.

[14] B. Engquist, A. Majda, Radiation Boundary Conditions for Acoustic and Elastic Wave Calculations, Commun. Pure Appl. Math. 32 (1979), 313–357. https://doi.org/10.1002/cpa.3160320303.

[15] B. Engquist, L. Ying, Sweeping Preconditioner for the Helmholtz Equation: Hierarchical Matrix Representation, Commun. Pure Appl. Math. 64 (2011), 697–735. https://doi.org/10.1002/cpa.20358.

[16] Y.A. Erlangga, Advances in Iterative Methods and Preconditioners for the Helmholtz Equation, Arch. Comput. Methods Eng. 15 (2007), 37–66. https://doi.org/10.1007/s11831-007-9013-7.

[17] Y.A. Erlangga, R. Nabben, On a Multilevel Krylov Method for the Helmholtz Equation Preconditioned by Shifted Laplacian, Electron. Trans. Numer. Anal. 31 (2008), 403–424.

[18] Y. Erlangga, C. Vuik, C. Oosterlee, On a Class of Preconditioners for Solving the Helmholtz Equation, Appl. Numer. Math. 50 (2004), 409–425. https://doi.org/10.1016/j.apnum.2004.01.009.

[19] Y. Erlangga, C. Vuik, C. Oosterlee, Comparison of Multigrid and Incomplete LU Shifted-Laplace Preconditioners for the Inhomogeneous Helmholtz Equation, Appl. Numer. Math. 56 (2006), 648–666. https://doi.org/10.1016/j.apnum.2005.04.039.

[20] Y.A. Erlangga, C.W. Oosterlee, C. Vuik, A Novel Multigrid Based Preconditioner for Heterogeneous Helmholtz Problems, SIAM J. Sci. Comput. 27 (2006), 1471–1492. https://doi.org/10.1137/040615195.

[21] M.J. Gander, I.G. Graham, E.A. Spence, Applying GMRES to the Helmholtz Equation with Shifted Laplacian Preconditioning: What Is the Largest Shift for Which Wavenumber-Independent Convergence Is Guaranteed?, Numer. Math. 131 (2015), 567–614. https://doi.org/10.1007/s00211-015-0700-2.

[22] M.J. Gander, L. Halpern, F. Magoulès, An Optimized Schwarz Method with Two-sided Robin Transmission Conditions for the Helmholtz Equation, Int. J. Numer. Methods Fluids 55 (2007), 163–175. https://doi.org/10.1002/fld.1433.

[23] M.J. Gander, F. Nataf, An Incomplete Lu Preconditioner for Problems in Acoustics, J. Comput. Acoust. 13 (2005), 455–476. https://doi.org/10.1142/s0218396x05002803.

[24] C. Geuzaine, GetDP: A General Finite-element Solver for the de Rham Complex, Proc. Appl. Math. Mech. PAMM 7 (2008), 1010603–1010604. https://doi.org/10.1002/pamm.200700750.

[25] C. Geuzaine, J. Remacle, Gmsh: A 3-D Finite Element Mesh Generator with Built-in Pre- and Post-processing Facilities, Int. J. Numer. Methods Eng. 79 (2009), 1309–1331. https://doi.org/10.1002/nme.2579.

[26] S. Gong, I.G. Graham, E.A. Spence, Domain Decomposition Preconditioners for High-Order Discretizations of the Heterogeneous Helmholtz Equation, IMA J. Numer. Anal. 41 (2020), 2139–2185. https://doi.org/10.1093/imanum/draa080.

[27] W.B. Gragg, The Padé Table and Its Relation to Certain Algorithms of Numerical Analysis, SIAM Rev. 14 (1972), 1–62. https://doi.org/10.1137/1014001.

[28] P. Hooghiemstra, D. van der Heul, C. Vuik, Application of the Shifted-Laplace Preconditioner for Iterative Solution of a Higher Order Finite Element Discretisation of the Vector Wave Equation: First Experiences, Appl. Numer. Math. 60 (2010), 1157–1170. https://doi.org/10.1016/j.apnum.2010.07.004.

[29] R. Kechroud, A. Soulaimani, Y. Saad, S. Gowda, Preconditioning Techniques for the Solution of the Helmholtz Equation by the Finite Element Method, Math. Comput. Simul. 65 (2004), 303–321. https://doi.org/10.1016/j.matcom.2004.01.004.

[30] Y.Y. Lu, A Complex Coefficient Rational Approximation of $\sqrt{1+x}$, Appl. Numer. Math. 27 (1998), 141–154. https://doi.org/10.1016/s0168-9274(98)00009-9.

[31] F.A. Milinazzo, C.A. Zala, G.H. Brooke, Rational Square-Root Approximations for Parabolic Equation Algorithms, J. Acoust. Soc. Am. 101 (1997), 760–766. https://doi.org/10.1121/1.418038.

[32] J. Nédélec, Acoustic and Electromagnetic Equations, Springer, New York, 2001. https://doi.org/10.1007/978-1-4757-4393-7.

[33] D. Osei-Kuffuor, Y. Saad, Preconditioning Helmholtz Linear Systems, Appl. Numer. Math. 60 (2010), 420–431. https://doi.org/10.1016/j.apnum.2009.09.003.

[34] Y. Saad, Iterative Methods for Sparse Linear Systems, SIAM, 2003. https://doi.org/10.1137/1.9780898718003.

[35] Y. Saad, M.H. Schultz, GMRES: A Generalized Minimal Residual Algorithm for Solving Nonsymmetric Linear Systems, SIAM J. Sci. Stat. Comput. 7 (1986), 856–869. https://doi.org/10.1137/0907058.

[36] H. Tal-Ezer, E. Turkel, The Iterative Solver RISOLV with Application to the Exterior Helmholtz Problem, SIAM J. Sci. Comput. 32 (2010), 463–475. https://doi.org/10.1137/08072454x.

[37] M. Taylor, Pseudodifferential Operators, Princeton University Press, 1991.

[38] L.L. Thompson, A Review of Finite-Element Methods for Time-Harmonic Acoustics, J. Acoust. Soc. Am. 119 (2006), 1315–1330. https://doi.org/10.1121/1.2164987.

[39] E. Turkel, Boundary Conditions and Iterative Schemes for the Helmholtz Equation in Unbounded Regions, in: F. Magoulès (Ed.), Computational Science, Engineering & Technology Series, Saxe-Coburg Publications, Stirlingshire, 2008: pp. 127–158. https://doi.org/10.4203/csets.18.5.

[40] I. Zangré, K. Lamien, L. Somé, O. Nakoulima, Phase Reduction Model for an Accurate and Costless Finite Elements Solution to High-Frequency Time-Harmonic Scattering Problems, Far East J. Appl. Math. 108 (2020), 41–66. https://doi.org/10.17654/am108010041.